RADIO DIRECTION FINDING

Radio direction finding is the technique of measuring radio wave angle of arrival (*AOA*), as illustrated in Fig. 1. A transmitting antenna radiates radio energy toward the direction finding site. At distances greater than ten wavelengths from the transmitting antenna, the radio wave can be represented as a plane wave, with linear contours of constant amplitude perpendicular to the direction of propagation. Ideally, the radiated energy propagates along the most direct path from the transmitter to the receiver. The receiving system is conventionally called a *direction finder*, or *DF* for short. Figure 1 shows AOA expressed in terms of an *azimuth* component in the horizontal plane and an *elevation* component measured in the vertical plane, relative to the horizon.

A direction finder employs one or more antennas in a *DF array*, used to detect the incoming radio wave. The output of each antenna is applied to a radio receiver, and this signal is sampled and input to a DF computer processor for determining AOA. The DF processor may either (1) determine the direction of energy flow toward the direction finder, (2) measure the direction of maximum rate of phase change across the DF array, or (3) estimate the direction of the velocity vector, normal to the plane wave fronts. A well-known example of a simple DF system, which is still in use, is a rotatable loop antenna connected to a radio receiver as shown in Fig. 2. AOA is measured by determining the direction of energy flow toward the DF antenna. This is accomplished by rotating the loop for minimum audible output as indicated by the headphones, and thereby placing the null response of the loop on the AOA of the received signal. Thus, the direction to the transmitter is indicated by the broadside angle of the loop. The loop also has a null response on the reciprocal bearing, 180° from the true AOA. This problem of ambiguity can be resolved with an auxiliary "sense antenna."

The advent of radio communication in the late 1890s launched the development of direction finding techniques for navigation and radio transmitter location. Radio navigation and radio location are complimentary technologies exploiting a common methodology. For example, signals received at sea from known shore-based radio beacons are used for navigation by *triangulation* to *fix* the position of a ship [Fig. 3(a)]. Conversely, two or more direction finders at known locations can be used to locate a radio transmitter by triangulation as shown in Fig. 3(b).

For location applications, the DF result is the observed *line of bearing* (*LOB*) or *bearing* to the transmitter. A LOB is expressed either as the *true bearing*, that is, an angle measured clockwise from true North, or as a *relative bearing* which is measured clockwise from a reference direction such as the heading of a mobile DF platform (ship, aircraft, vehicle). True bearings are generally used to locate a radio transmitter on a map.

A major factor affecting DF system performance is the process of *confirming* that each reported bearing is associated with the correct signal. Since there may be many signals on the air with overlapping frequencies, confirmation is sometimes a very difficult task. Often the achievable accuracy of a DF net is determined by the reliability with which each bearing is confirmed to be associated with the correct signal.

Operational DF measurements are always subject to error, and minimizing DF error is a major consideration in direction finder system design. DF error may be divided into three categories:

1. **Site error** is caused by reradiating structures and ground plane characteristics at the DF antenna site which distort the arriving wavefronts into nonplanar configurations. Under these conditions the estimated AOA will vary depending on the location of the DF antenna array in the wavefield.

2. **Measurement error** may be caused by imperfections in the DF system instrumentation but it is more frequently due to perturbed conditions in the received wavefield. Multipath propagation and cochannel interference create a multicomponent wavefield and are common sources of error in DF algorithms that are based on a single plane wave model. Multipath occurs when the signal arrives at the DF site via two or more propagation paths. Cochannel interference is caused by other on-the-air signals transmitted at frequencies that overlap the signal of interest.

3. **Propagation error,** the most fundamental source of error, is introduced by the propagation medium which may deviate the radio wave off the most direct path to the DF receiver. At best, the DF system accurately measures AOA *as received at the DF site*, and the estimated bearing may not indicate the "true" direction to the transmitter. Propagation error, which is beyond the control of the DF system engineer, imposes a fundamental limit to achievable DF accuracy.

Conventional shipboard DF operations in the high frequency band (2 to 30 MHz) illustrate all of these DF errors in a single situation (Fig. 4). Signals experience multipath propagation through the ionosphere. Also, the ionosphere introduces propagation error by deviating each of the arriving propagation modes out of the great circle plane. A conventional single plane wave DF algorithm produces DF error by treating the superimposed ionospheric modes as a single plane wave. Finally, the ship's superstructure introduces additional site error by reradiating the incident waves into the DF array, thus creating a second and more complex source of multipath.

This brief introduction has provided an overview of the science and technology of radio direction finding. For a more thorough overview of the field, the interested reader is referred to Refs. (1–3). An extensive bibliography of direction finding literature is provided in Ref. (4). The following sections discuss various approaches to DF system design. Conventional DF design techniques based on the assumption of a single incident plane wave signal are considered. The impact of operational conditions on conventional DF system performance is emphasized along with important methods for mitigating site error. Also, modern design techniques are described which are based on the decomposition of multicomponent wavefields. These DF tech-
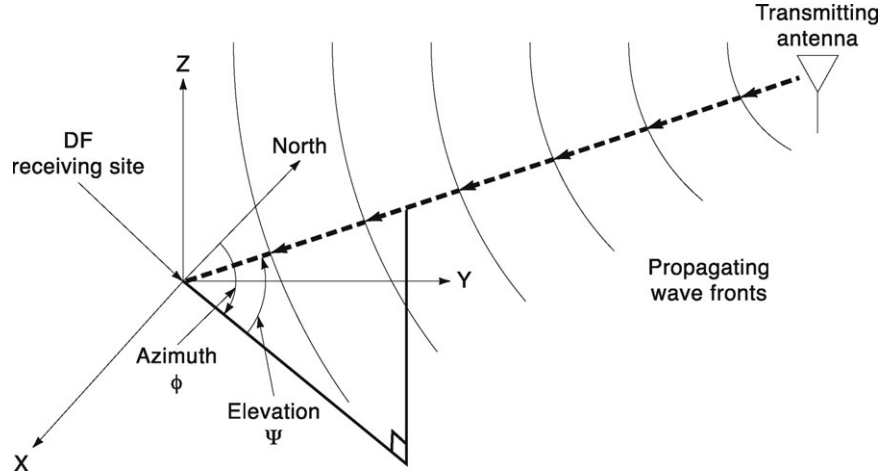
Figure 1. Radio wave received at a direction finding site. Contours of constant amplitude propagate radially from the transmitting antenna, and the angle-of-arrival is characterized by azimuth and elevation.
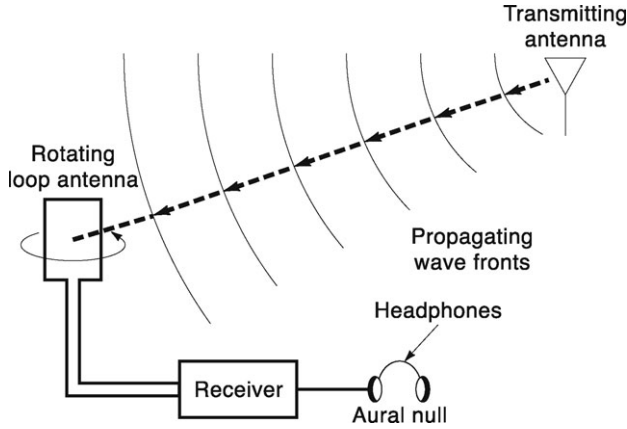

Figure 2. Rotating simple loop antenna direction finding system. The headphones are used to detect when the AOA is broadside to the loop and the received signal is minimum.

niques are generally referred to as superresolution methods. Finally, current trends in DF research are surveyed and performance benefits are assessed.

APPLIED DIRECTION FINDING TECHNOLOGY

A radio direction finding system performs both time and spatial sampling of the field distribution and processes the samples to estimate AOA. A DF system acquires spatial samples through a combination of individual antenna placements and/or antenna patterns. The local description of any spatial field distribution may be estimated either from a set of spatially separated samples or from a set of spatial derivatives at a single point in space.

A local description of a field at an arbitrary point $\mathbf{r}$ in a Cartesian coordinate system may be developed by considering a monochromatic plane wave propagating in free space as

$$x(t, r) = B \exp[j2\pi(f_o t + \mathbf{k}_o \cdot r) + \gamma] \tag{1}$$

where $\mathbf{r} = (r_x, r_y, r_z)$ is the spatial coordinate, B is signal amplitude, f_o is the frequency of the wave, $\mathbf{k}_o = \mathbf{v} f_o / |\mathbf{v}|^2$ is the wavenumber which is a function of the scalar frequency and $\mathbf{v}$ is the vector velocity of propagation (typically assumed to be the speed of light in free space), and γ is a random starting phase which is uniformly distributed over [0, 2π]. The AOA information is contained in the $2\pi \mathbf{k}_o \cdot \mathbf{r}$ phase term and is given as

$$2\pi \mathbf{k}_o \cdot \mathbf{r} = \beta(r_x \cos\phi\cos\psi + r_y \sin\phi\cos\psi + r_z \sin\psi)$$
$$\beta = 2\pi|\mathbf{k}_o| = 2\pi/\lambda_o$$
$$\lambda_o = \mathbf{wavelength} \tag{2}$$
$$\phi = \mathbf{azimuth\ AOA}$$
$$\psi = \mathbf{elevation\ AOA}$$

If it is assumed that there are M antennas in the array, then a simultaneous sampling of the output at each antenna may be expressed as a column vector $\mathbf{X}(t, \mathbf{r}) = [x_1, \ldots, x_M]^T$, where T denotes the transpose operation. The vector $\mathbf{X}$ is known as an *array snapshot*. If the AOA term in Eq. (1) is separated, then the array snapshot for a single incident signal may be characterized as

$$\mathbf{X}(t, r) = \mathbf{A}(r)s(t) + \mathbf{N}(t) \tag{3}$$

where $s(t) = B \exp(j2j\pi f_o t + \gamma)$ is the time varying part of the signal, and the thermal noise in each receiving channel is represented by $\mathbf{N}(t) = [n_1, \ldots, n_M]^T$. $\mathbf{A}(r)$ is an M × 1 column vector which represents the antenna array response for a signal arriving from an arbitrary direction (ϕ, ψ) as

$$\mathbf{A}(r) = [a_1, \ldots, a_M]^T$$
$$a_i = \exp(j2\pi \mathbf{k}_o \cdot r_i) \tag{4}$$

for an array of isotropic antennas. The column vector given by Eq. (4) is referred to as the *array steering vector*. The collection of all array steering vectors as a function of AOA, polarization, and frequency is referred to as the *array manifold*.

Two examples of wavefield sampling are shown in Fig. 5. Figure 5a illustrates an aerial view looking down on the surface of the Earth at a single plane wave propagating
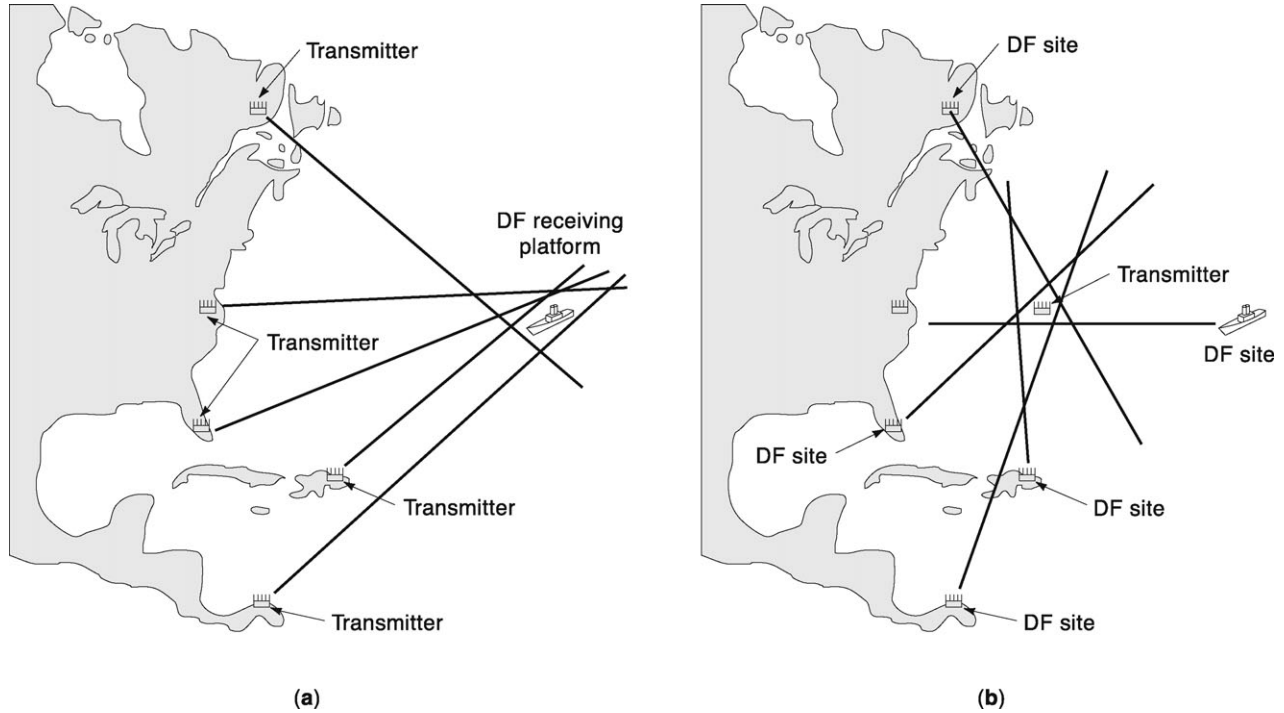
(a)   **(b)**

Figure 3. Similarity of radio navigation and DF radio-location technology. (a) Shipboard navigation technique using five radio beacons for position fixing. (b) Radio transmitter location technique with five direction finding sites.
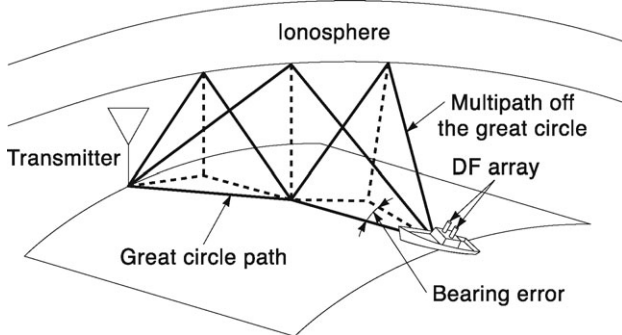

Figure 4. Shipboard direction finding scenario illustrating sources of bearing error. An error will result from the fact that the radio wave is not traveling on a direct path from the transmitter. The presence of multiple signals will induce a measurement error due to wave interference, and the metallic structure of the ship will cause errors due to reflections near the receiving antenna.

across a circular array of eight antennas. In this case, the amplitude term B Eq. (1) is constant throughout the space. The phase term $2\pi(f_o t + \boldsymbol{k}_o \cdot \boldsymbol{r}) + \gamma$ is illustrated for constant contours of $n\pi$ as a function of $\boldsymbol{r}$. The contours plot as parallel straight lines, and AOA is orthogonal to the contours of constant phase. In the example plot of Fig. 5b, it is assumed that four signals are propagating across an interferometer array of seven antennas. The signals are of equal amplitude and are assumed to be arriving from azimuth and elevation AOAs of $(45°, 15°)$, $(50°, 30°)$, $(60°, 45°)$, and $(45°, 50°)$ respectively. In this case, the amplitude of the composite signal is not constant but varies with $\boldsymbol{r}$. The dark contours illustrate those regions where the composite am-

plitude exceeds a normalized threshold of 0.95 units. The thin lines are contours of constant phase showing a somewhat distorted pattern. Clearly, the antenna array is not able to adequately sample all the features of the spatial interference pattern and a plane wave solution will incur multipath error; decomposing the wave field into its individual components is required for a complete DF solution.

The processing objective of radio direction finding is to determine a unique AOA which is consistent with the set of data measured on the array. The key to this process is a knowledge of the array manifold *that includes site effects of the operational environment*. In the most general form, the bearing estimation process requires an iterative comparison between the observed data and the array manifold for every possible combination of polarization and AOA.

The remainder of this section describes DF techniques that progress from simple closed-form solutions (where stringent constraints apply to the antenna patterns, array geometry, local scattering environments, and number of simultaneous signals), to more general calibration based DF processing algorithms, and finally to DF methods that decompose multisignal wave fields.

Single Plane Wave Direction Finding

Direction Finding in the Absence of Site Effects. Traditional direction finding techniques assume a single uniform plane wave incident upon the DF antenna array. These DF techniques require noninvasive electromagnetic field measurements across a region in space in which the wave front must maintain its properties as a uniform plane wave. This requirement imposes stringent constraints on the installation site, on the selection of the antenna ele-
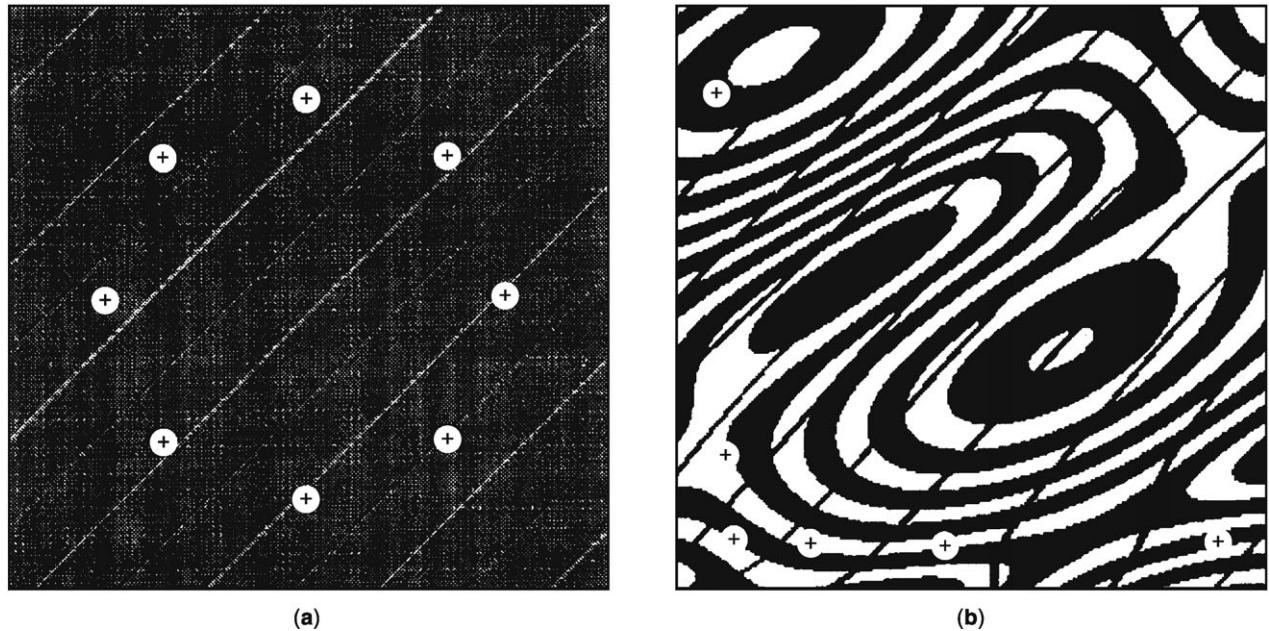
Figure 5. Contrasting single and multiple plane wavefields incident on DF arrays. (a) Single plane wave incident on a circular array of antennas. Amplitude is everywhere constant and contours of constant phase are parallel straight lines. (b) Multiple plane waves incident on orthogonal baseline interferometer array. Contours of constant amplitude and phase are distorted. (Contour plot provided by D. N. Travers.)

ments, on the array geometry, and in some cases on the class of signals against which the system can operate. The requirement that the system be noninvasive demands that (1) no antenna element within the array perturbs the response characteristics of any other antenna element (i.e., mutual coupling must be negligible) and (2) the array of antennas must be installed in a region that is sufficiently separated from structures which would disturb the planarity property of the propagating wave. The selection of array geometry, choice of antenna elements, and site selection are all design factors that influence the simplicity of the DF process and system performance for various signal conditions (e.g., signal-to-noise ratio [*SNR*], polarization, elevation).

If the noninvasive constraints are satisfied and simple antenna elements are deployed in a favorable array geometry, then the characteristic response of the system (array manifold) may be analytically predicted as a function of AOA and polarization. In this case, AOA may be calculated by closed-form analytic solution, thus avoiding the more general requirement for an iterative search. For example, solution of Eq. (2) for phase measurements made among identical elements in a circularly disposed antenna array (*CDAA*) produced an estimate of AOA using a closed-form arctangent solution. Many CDAA closed-form processing techniques relax the mutual coupling constraint among the antenna elements, provided array rotational symmetry is preserved.

Eleven examples of traditional DF systems that are based on the assumption of a single uniform plane wave incident upon the antenna array are listed in Table 1. The table summarizes antenna array configuration, basis for AOA determination, primary advantages and disadvan-

tages, and provides literature references to more detailed descriptions. Table 2 illustrates the corresponding antenna array geometries and analytic processing algorithms associated with the eleven examples of Table 1. DF results are derived from solutions of Eqs. 1 and 2 with appropriate modifications to account for antenna patterns and array geometry.

Under more general conditions, it may not be possible or desirable to impose the restrictive design constraints that are essential for traditional DF techniques. Under more general installation conditions, arbitrary and diverse antenna elements that experience mutual coupling are installed in irregular array geometries (sometimes dictated by the site) on a location that distorts the characteristics of the incident uniform plane wave. Under these conditions, the DF process must be generalized to perform an iterative comparison between the observed response vector and the array manifold to determine AOA. Further, calibration measurements to determine installed antenna response patterns are required to characterize the array manifold as a function of AOA (and polarization). DF calibration and its application to iterative DF processing are discussed in the next section.

DF Under Conditions of Site Interaction. The previous discussion focused on DF systems that were isolated from electrically conducting structures, and each antenna element within the array was excited by a single, uniform plane wave. However, an incident wave induces currents on conducting structures in the vicinity of the array, and these induced currents become sources of secondary radiation which are also coupled into the DF antennas. In the presence of conducting structures, DF antennas experience

Table 1. Examples of Traditional DF Systems

DF System	Typical Array Description (See Table 2 for Array Geometry)	Basis of Operation	Primary Advantages	Primary Limitations	References
Rotatable loop	Single, rotatable loop	Determines orientation of horizontal component of curl of electric field vector	Simple processing, small antenna size	Polarization error	Franks (5)
Crossed loops	Orthogonal pair of fixed, horizontal-axis loops				
Rotatable H-Adcock	Pair of identical, vertical electric dipoles, differentially connected	Responds to horizontal spatial derivatives of vertical electric field vector	Avoids polarization error by responding only to vertical polarization	Reduced sensitivity over loop	Jenkins (2)
Four element Adcock array	Four element, mast-mounted array of vertical electric dipoles, differential connection of diametrically opposite element pairs				
Spinning spaced loop	Coaxial pair of identical loops, differentially connected	Responds to horizontal spatial derivatives of horizontal magnetic field vector	Responsive to all polarizations, without polarization error	Reduced sensitivity over loop	Travers (6) Hipp (7)
Fixed, crossed spaced loop	Four, crossed spaced loops				
Phase-sampled linear interferometer	Two linear arrays of identical antenna elements	Measures phase gradient	Reduced noise-induced DF error Phase-only process	Requires large, clear site	Kennedy, Wharton (8)
Phase-sampled pseudo-doppler	CDAA of linear monopoles or dipoles			Sensitive to phase errors	Hipp (9)
Wullenweber	CDAA of multiple vertical elements in presence of cylindrical reflecting screen	Develops high gain, rotating beam pattern	High sensitivity, good interference rejection	Requires large, clear site	Wundt (10)
Amplitude mode	CDAA of identical antenna elements	Develops various orders of spatial derivatives in horizontal plane	Higher order patterns tend to be less sensitive to site interaction	Higher order patterns are less sensitive to low-level signals	Davies (11)
Phase mode	CDAA of identical antenna elements	Develops various orders of spatial derivatives in horizontal plane	DF processing reduces to measuring a phase difference	Directly sensitive to phase errors	Davies (11)

phase and amplitude perturbations that distort their ideal patterns. If one assumes ideal array patterns, these distortions result in erroneous DF estimates. To the extent that the structures remain stationary, the distorted antenna patterns and the erroneous DF estimates are repeatable functions of the incident signal AOA, polarization, and frequency. This repeatable characteristic provides the basis for using calibration measurements to improve DF performance under conditions of stationary site interaction.

Calibration measurements to accommodate site interaction can be performed at either of two levels: (1) measurement of AOA error correction values or (2) measurement of installed antenna response patterns. The application and effectiveness of these two basic approaches for DF operation in the presence of site interaction are the focus of the following paragraphs. Under either scenario, the basic procedure for performing the calibration is to record the appropriate measurement from the *installed* DF system while exposing it to a controlled (calibration) incident plane wave under every appropriate combination of signal parameter (i.e., azimuth, elevation, polarization, and/or frequency).

Calibration for AOA Error Correction. For a low degree of residual site interaction with the DF antennas, moderate pattern distortion and moderate DF error exist. In this case, calibration for AOA error correction is effective. One conventional approach for reducing AOA errors in DF performance is to start with a carefully controlled site in which the DF array is removed as far as practical from

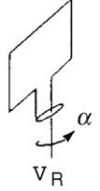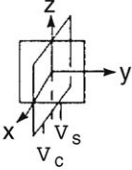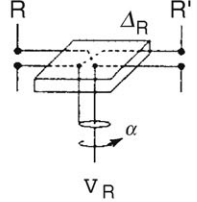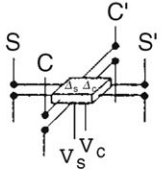Table 2. Traditional DF Array Geometries and Algorithms
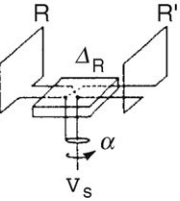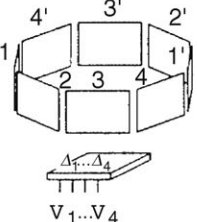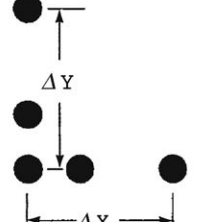
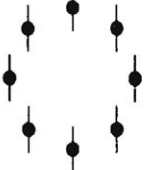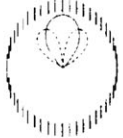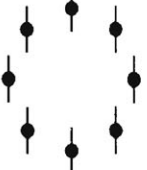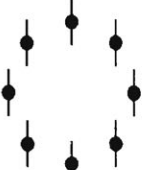| DF System	Typical Array Configuration	DF Algorithm (ϕ = Azimuth AOA, Ψ = Elevation AOA)
Rotatable loop		Operator monitors both the loop response V_R and the orientation α of the loop while rotating the loop to identify the response null from a vertical polarization response pattern described by $V_R(\alpha) \propto \sin(\phi - \alpha)$
Crossed simple-loops		$\phi = \tan^{-1}\dfrac{V_s}{V_c}$
Rotatable H-Adcock		Operator monitors both the H-Adcock response V_R and the azimuth orientation α of the H-Adcock array while rotating the array to identify the response null from a response pattern described by $V_R(\alpha) \propto \sin(\phi - \alpha)$
Four element Adcock array		$\phi = \tan^{-1}\dfrac{V_s}{V_c}$
Spinning spaced loop		Operator monitors both the spaced-loop response V_R and the orientation α of the spaced-loop array while rotating the array to identify the stable response null from a response pattern described by $V_R(\alpha) \propto [E_H \sin\Psi \sin(\phi - \alpha) - E_V \cos(\phi - \alpha)]\cos\Psi \sin(\phi - \alpha)$ where E_V and E_H are respectively the vertically and horizontally polarized components of the incident electric field
Fixed, crossed spaced loop (for spaced loops illustrated)		$A_0 = (V_1 + V_2 + V_3 + V_4)/4$ $A_2 = (V_1 - V_3)/4$ $B_2 = (V_2 - V_4)/4$ $D = \pm(A_2^2 + B_2^2 - A_0^2)^{1/2}$ $S2 = -(A_2 D + B_2 A_0)/(A_0^2 + D^2)$ $C2 = -(A_2 A_0 - B_2 D)/(A_0^2 + D^2)$ $\phi = \frac{1}{2}\tan^{-1}(S2/C2)$
Phase-sampled linear interferometer		Use unambiguous phase measurements from short baselines to resolve the ambiguities in the phases $\Delta\Phi_x$ and $\Delta\Phi_y$ measured across the two long baselines ΔX and ΔY. Use the resolved phase measurements $\Delta\Phi_x$ and $\Delta\Phi_y$ to estimate the azimuth and elevation AOA $\phi = \tan^{-1}\left(\dfrac{\Delta\Phi_y/\Delta Y}{\Delta\Phi_x/\Delta X}\right)$ $\psi = \cos^{-1}\left[\dfrac{c}{\omega}\sqrt{\left(\dfrac{\Delta\Phi_x}{\Delta X}\right)^2 + \left(\dfrac{\Delta\Phi_y}{\Delta Y}\right)^2}\right]$

Table 2. (*Continued*)

DF System	Typical Array Configuration	DF Algorithm (ϕ = Azimuth AOA, Ψ = Elevation AOA)
Phase-sampled pseudodoppler		Resolve the ambiguous phase measurements to assure that phase differences between adjacent elements remain less than 180° in magnitude. Compute the Fourier series coefficient A_1 and B_1 for the first harmonic of the resolved phase progression around the circle. Solve for the azimuth AOA $\phi = \tan^{-1}(B_1/A_1)$
Wullenweber		Develop a pair of rotating high-gain beams to produce a rotating beam pattern having a deep pattern null in the steering direction and a rotating beam pattern having a high gain pattern maximum in the steering direction
Amplitude mode		Combine every individual response v_n from CDAA element located at orientation α_n to develop responses proportional to the sine/cosine Fourier series coefficients A_m and B_m for the mth harmonic of the directional response around the array. $A_m = \Sigma\, v_n \cos(m\alpha_n)$ $B_m = \Sigma\, v_n \sin(m\alpha_n)$ Calculate the unambiguous azimuth AOA using two adjacent modes $\phi = \tan^{-1}\left(\dfrac{B_{m+1}}{A_{m+1}}\right) - \tan^{-1}\left(\dfrac{B_m}{A_m}\right)$ for $m \geq 0$ In the absence of intrinsic polarization error, an ambiguous AOA may be calculated from a single mode as $\phi = \dfrac{1}{m}\tan^{-1}\left(\dfrac{B_m}{A_m}\right) + i\dfrac{\pi}{m}, i = 0, 1, \ldots m \quad$ for $m > 0$
Phase mode		Develop responses proportional to the exponential Fourier series coefficients a_m for the mth harmonic of the directional response around the array. $a_m = \Sigma\, v_n\, e^{-jm\alpha_n}$ The azimuth AOA is estimated as the phase difference between the responses of two adjacent phase mode responses $\phi = \Phi(a_m) - \Phi(a_{m-1})$

perturbing structures. To the extent that this objective can be achieved, AOA errors due to site interaction are minimized. In this situation, a reasonably good AOA approximation is obtained using the single plane wave assumption, and residual AOA error due to site interaction is reduced through a calibration correction curve.

A primary criterion for AOA error correction to be effective is that the curve of corrected bearing versus observed bearing (i.e., the uncorrected AOA estimated by the DF system) is single valued. Figure 6 shows two calibration correction curves illustrating both moderate and severe AOA error. The calibration curve of Fig. 6(a) shows a moderate case of site interaction and a single valued AOA correction curve. The calibration curve of Fig. 6(b) illustrates the impact of severe site interaction and displays

reentrant regions. There are two intervals in which one value of observed bearing estimated by the DF system is associated with more than one corrected bearing. Calibration for AOA errors is not effective in reentrant regions, and experimental determination of the array manifold is generally necessary.

Calibration of antenna responses. DF is a process that requires a priori knowledge of the installed array steering vectors. Conventional DF system development assumes a carefully controlled array of antennas having response patterns that are closely approximated by ideal predictions. When the DF array is installed on an adverse site, antenna patterns can suffer severe distortion from nearby conducting structures. In such cases, required knowledge of the installed array steering vectors must be obtained by
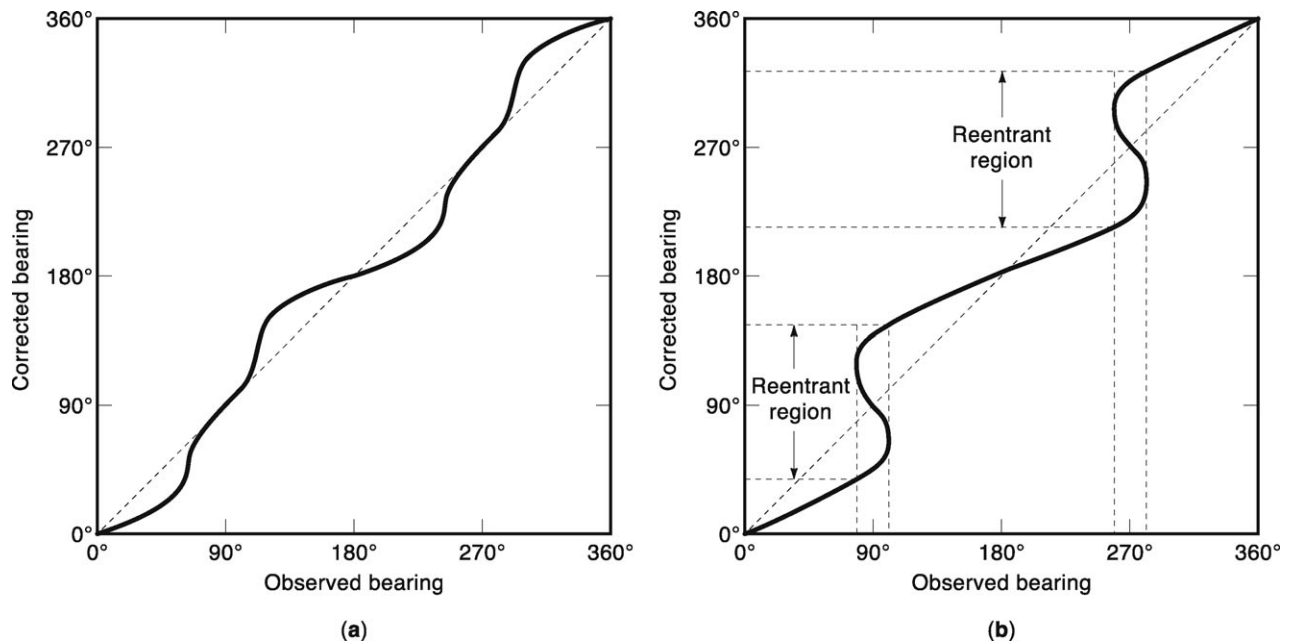
Figure 6. Moderate and severe site interaction AOA calibration curves. (a) Moderate site interaction with AOA errors which are correctable. (b) Severe site interaction with reentrant regions in which AOA error correction is ambiguous.

measuring antenna responses and storing this information in an array manifold consisting of antenna patterns versus frequency, AOA, and polarization. For ship and aircraft platforms, the installed array steering vectors may be measured by repeatedly turning the platform in circles to expose the antennas to all possible AOAs from a farfield calibration station transmitting a wide range of signal frequencies. As an alternative, array manifolds have been obtained by performing calibrationlike measurements of antenna responses from scale-model arrays installed on highly detailed miniature models of the platform.

Iterative Search DF Techniques. The essential process of any iterative search DF technique is to select the AOA of the calibrated array steering vector which *best* agrees with the unknown measured array response. The primary difference between DF iterative search schemes is the criterion for obtaining best agreement. A commonly used procedure for iteratively comparing observed array response to the calibrated array response vectors is a beam steering process which acts as an equivalent bank of matched filters. In this case, best agreement is defined in a least mean squared sense.

A digital beamformer may be viewed as a matched filter that processes the observed antenna response to produce a single (scalar) response that is maximum when the preferred direction of the beamformer best agrees with the AOA of the signal. Beam steering DF iteratively processes an observed response vector through a progression of matched filters (viz., array steering vectors), each of which represents a different AOA. Under the constraint of a normalized input vector (i.e., unit-norm), the output level of the filter is maximum when excited by a vector that matches the filter parameters. Or stated another way, maximum output is obtained from the filter whose steer-

ing vector AOA best agrees with the bearing of the observed signal. In this manner, the process scans (or steers) a simulated beam over all possible AOAs, searching for the steering direction that maximizes the beamformer response.

The beam steered iterative process may be characterized mathematically by considering an array manifold of L steering vectors for a particular frequency. The array manifold is the set of array steering vectors $\boldsymbol{A}$ for $i = 1, L$. This implies that the DF system was calibrated at L bearings in the interval [0, 360] degrees. If $\overset{a}{X}$ denotes the observed array response vector for a signal of interest, then the output y of each matched filter is given as

$$y_i = |\boldsymbol{A}_i^{\mathrm{H}}\hat{\boldsymbol{X}}|, \quad i = 1, L \tag{5}$$

where H denotes the Hermitian or conjugate transpose operation. The best AOA estimate is obtained when y_i is a maximum. A typical plot of y is shown in Fig. 7. In this illustration, $L = 25$, and the AOA estimate is $195°$ corresponding to the maximum value associated with the array steering vector at y_{14}. This process results in an AOA estimate that is best in a least squared sense.

Three areas of particular importance that impact the performance of DF systems which are based on iterative search techniques are (1) antenna array design, (2) adequacy of calibration, and (3) polarization effects. Antenna array design critically influences the pattern of the steerable beam. The characteristics of the steerable beam are determined by the geometry of the array, the intrinsic element patterns and the number of antennas in the array. Of primary concern in the design of the steerable beampattern is the beamwidth of the main lobe and relative level of the side lobes.

Beam steering DF system performance is also controlled by the accuracy and completeness of the calibration process
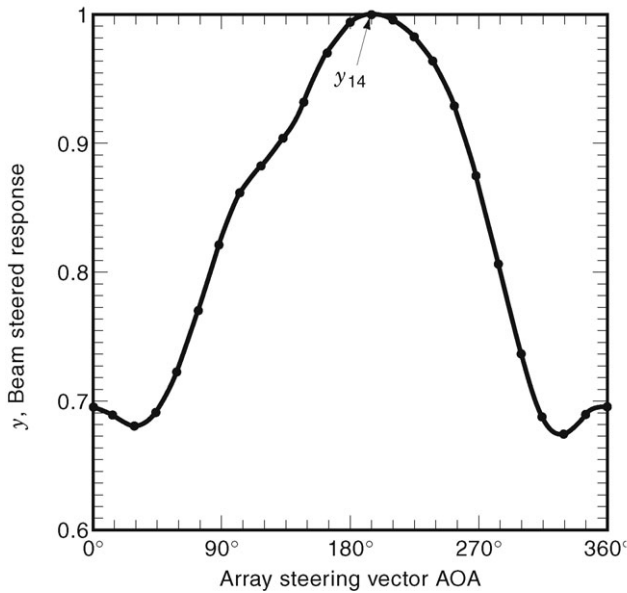
Figure 7. Beam steered iterative search indicating a maximum when steering angle matches AOA of arriving signal.

used to characterize the array manifold. To obtain robust maxima in the matched filtering process, the array manifold should be acquired at high SNR to minimize the possibility of contaminated data. The calibration data must be measured in AOA increments that permit accurate interpolation.

The array manifold varies not only with AOA, but also with signal polarization. Under arbitrary polarization conditions, the steering vector must be adjusted to match the polarization *and* the AOA of the incident signal. For arbitrary polarization applications, the array manifold at each steering direction must consist of a pair of steering vectors for two different polarizations, for example, $A_V (\phi, \psi)$ and $A_H (\phi, \psi)$ for vertical and horizontal polarization. The additional maximization step required by the polarization extension of beam steering DF at each bearing is to maximize the beamformer response over all possible linear combinations of $A_V (\phi, \psi)$ and $A_H (\phi, \psi)$. The matched filter thus becomes a digital beamformer that processes the observed antenna response producing a single (scalar) response that is maximum when the steered direction of the beamformer matches the AOA of the received signal.

DF Error Mitigation

There are a number of sources of error in radio direction finding, and an exhaustive discussion is well beyond the scope of this survey; however, there are three categories common to all DF systems: (1) site errors, (2) measurement errors, and (3) propagation errors. These are considered in the following discussion.

Site Errors. The antenna array generally designed to operate on a site that is clear of obstructions and reradiating structures. As discussed in the previous section, array calibration is generally used to mitigate site error in those cases where the DF antenna must operate in a cluttered

environment. The concern in this section is selecting a site that least perturbs the incident signal.

Generally, DF systems are deployed on level, unobstructed terrain where the ground dielectric constant and conductivity are reasonably uniform within 10 to 20 wavelengths of the antenna array. Abrupt discontinuities in the electrical properties of the terrain such as nearby rivers, lakes, or coastlines should be avoided. Also DF sites in the vicinity of rock or mineral outcroppings are undesirable. Abrupt changes in terrain topology such as nearby mountains, high cliffs, or deep ravines should be avoided.

In addition to selection of natural features, proximity to manmade reradiating structures should also be considered. The DF site should be clear of above ground conductors such as utility lines and wire fences. The site should not have buried conductors beneath the antenna array such as pipelines or utility distribution lines. The site should be clear of tall structures such as buildings, bridges, or water towers.

It is rarely possible to achieve all of these conditions at a DF site. Generally, there are a number of other antennas deployed at a DF site, as well as buildings and facilities which support other signal intelligence gathering activities. In practice, the DF system engineer attempts to locate the antenna array on a site which contains fewest perturbing factors.

Measurement Errors. Leaving aside instrumental accuracy and resolution determined by SNR, significant DF measurement errors are caused by multipath and cochannel wave interference, which tends to corrupt the planarity of an incident wavefront. Two approaches for mitigating measurement errors are: (1) acquire data under favorable conditions and exclude corrupted data, and (2) extract the desired signal from the interference.

The first class of techniques includes wavefront tests which determine whether a single plane wave is present or if the wavefield is corrupted by interference. A test which has been used in *CDAA* systems is to compare the array scan of amplitude versus azimuth with an ideal sum or difference array response (1). In the case of the sum beam response, one tests for a symmetrical main lobe having an expected width depending upon frequency. When this condition is satisfied, it is assumed that a single planewave is present and the bearing data are accepted; otherwise, the bearing data are rejected. Another test which has been used successfully in interferometer systems is that of a linear phase progression across the array (12). If the wavefield consists of a single planewave, then the relative phase between separated antennas is linearly dependent upon distance. In the presence of wave interference, this condition is generally not satisfied.

The second class of techniques includes Fourier analysis (FFT) methods which decompose the received signal into highly resolved spectral bins. In many cases, interference due to other on-the-air signals may be separated from the desired signal through a difference in spectral occupancy. In this situation, accurate DF results may be obtained by DF processing each spectral bin occupied by the signal of interest and ignoring the spectral bins corrupted by the interfering signal. Another approach is to

use the superresolution techniques described in the next section. These techniques decompose the wavefield into its constituent components and permit accurate DF for each component of the wavefield.

Propagation Errors. DF error caused by propagation off the great circle path is essentially beyond the control of the system designer. In this case, the signal arrives at the antenna array from a direction that is not on the direct path to the transmitter. An example is a cellular telephone signal, propagating in a dense urban environment, received after reflection from several buildings. The received AOA may be considerably different from the true bearing to the transmitter. Another example is the refractive error introduced by the ionosphere on HF ionospheric paths (3).

The essential approach to minimimze the effect of off-path DF errors is to perform DF on the first arriving signal. One method for implementing this technique is to acquire data on the leading edge of the waveform after a signal off-to-on transition and before the multipath components arrive. Another alternative is to decompose the complex wavefield and identify the first arriving signal through cepstral delay analysis (13). In both implementations, the intent is to estimate AOA for the first arriving signal on the premise that it will most nearly represent the true bearing to the transmitter.

A technique which has been developed to mitigate off-path errors for HF skywave signals is that of elevation angle discrimination. This technique is based on the premise that signals arriving at higher elevation angles spend more time in the ionosphere and are therefore more prone to off-path refraction than are signals arriving at lower elevation angles. In those cases where multipath propagation is present, the mode arriving at the lower elevation angle produces an azimuth estimate closer to the great circle bearing than a higher angle mode. This situation is almost always true in practice. The limiting case is a surface wave with a simultaneous skywave component over a path at sea. The surface wave invariably produces a more accurate bearing estimate.

Superresolution Direction Finding Methods

DF techniques described in the previous section were primarily concerned with system response to a single component wavefield. In contrast, the problem considered in this section is that of decomposing a multicomponent wavefield. Superresolution methods are particularly attractive for solving the multicomponent problem since the wavefield is generally undersampled in the spatial domain. That is, the dimensions of the antenna array are small relative to the scale of the spatial interference pattern.

An important building block used in superresolution spectrum anaysis is the spatial covariance matrix. If the vector $\boldsymbol{X}$ denotes an array snapshot at time t_0, then $\boldsymbol{X}(t_0, \boldsymbol{r}) = [x(\boldsymbol{t}_0, \boldsymbol{r}_1), x(\boldsymbol{t}_0, \boldsymbol{r}_2), \ldots, x(\boldsymbol{t}_0, \boldsymbol{r}_M)]^T$ and for M antennas,

the spatial covariance matrix is given as

$$\boldsymbol{R} = \begin{bmatrix} R(\boldsymbol{r}_1, \boldsymbol{r}_1) & R(\boldsymbol{r}_1, \boldsymbol{r}_2) & \cdots & R(\boldsymbol{r}_1, \boldsymbol{r}_M) \\ R(\boldsymbol{r}_2, \boldsymbol{r}_1) & R(\boldsymbol{r}_2, \boldsymbol{r}_2) & \cdots & R(\boldsymbol{r}_2, \boldsymbol{r}_M) \\ \vdots & \vdots & \ddots & \vdots \\ R(\boldsymbol{r}_M, \boldsymbol{r}_1) & R(\boldsymbol{r}_M, \boldsymbol{r}_2) & \cdots & R(\boldsymbol{r}_M, \boldsymbol{r}_M) \end{bmatrix}$$

$$= E\{\boldsymbol{X}(t, \boldsymbol{r})\boldsymbol{X}^{\times}(t, \boldsymbol{r})\}$$

(6)

where H is the Hermitian operation and $E\{\cdot\}$ denotes statistical expectation. Each matrix element $R(\boldsymbol{r}_i, \boldsymbol{r}_j)$ is the averaged product of the output of the antenna located at point $\boldsymbol{r}_i$ times the conjugated output of the antenna located at point $\boldsymbol{r}_j$.

Subspace Based Superresolution. A large volume of work has been presented over the past two decades on superresolution techniques that are based on an eigen decomposition of the spatial covariance matrix. Many modern algorithms have their origin in the early work of Pisarenko (14) which was revived and expanded by Schmidt (15). Schmidt's MUltiple SIgnal Classification (*MUSIC*) algorithm is the most widely cited superresolution technique in the present day literature. It has been the springboard for a seemingly endless flow of methods that are variations of the original approach. In this treatise, the original MUSIC algorithm is considered; however, for an extensive survey of MUSIC related techniques, the reader is referred to Krim and Viberg (16).

The initial step in the MUSIC algorithm is to solve the following eigen equation

$$\boldsymbol{RE} = \lambda\boldsymbol{E} \tag{7}$$

where $\boldsymbol{R}$ is the $M \times M$ spatial covariance matrix, λ is an arbitrary eigenvalue, and $\boldsymbol{E}$ is an arbitrary eigenvector. This formulation implicitly assumes that the noise background is uncorrelated white Gaussian noise. The n eigenvalues may be ordered such that $\lambda_M \geq \lambda_{M-1} \geq \cdots \geq \lambda_1$. The corresponding eigenvectors are arranged to form the matrix $\boldsymbol{R}_E$

$$\boldsymbol{R}_E = [E_M, E_{M-1}, \ldots, E_1] \tag{8}$$

A threshold value is determined such that the eigenvalues greater than the threshold are assumed to be associated with eigenvectors residing in the signal subspace. Likewise, eigenvalues that are smaller than the threshold produce eigenvectors which are assumed to be in the noise subspace. If the spatial covariance matrix were $M \times M$ and there were d signals in the wavefield, then the resulting eigenvector matrix would be partitioned such that the first d columns are vectors spanning the signal subspace, and the rightmost $p = (M - d)$ columns are vectors spanning the noise subspace. If the matrix partition corresponding to noise were denoted $\boldsymbol{R}_p$, then the MUSIC spectrum would be given by

$$P = (\boldsymbol{A}^H \boldsymbol{R}_p \boldsymbol{R}_p^H \boldsymbol{A})^{-1} \tag{9}$$

where $\boldsymbol{A}$ is the $M \times 1$ array steering vector defined in the previous section. AOA is determined using an approach similar to the technique described in the previous section on iterative search methods. A scalar value P is computed
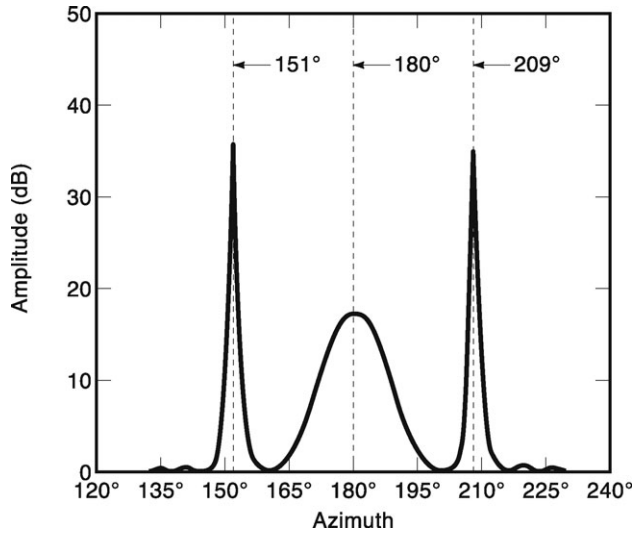
Figure 8. Two signals incident on a linear antenna array that were resolved using the MUSIC superresolution algorithm. The signals are received from azimuths of 151° and 180°, and the peak at 209° is an ambiguity. The peak at 180° is somewhat smeared due to the fact that the AOA of the signal is aligned with the longitudinal axis of the array (or end fire).

Figure 9. Two unresolved signals arriving from azimuths of 160° and 164° on a linear antenna array. The peaks at 196° and 200° are due to ambiguities in the array. In this case the effective aperture of the array was too small to resolve an AOA separation of 4°. A possible solution would be to lengthen the array by adding more antennas.

using Eq. (9) for each array steering vector A, and AOA is given by the array steering vector that maximizes P. If multiple signals were present in the incident wavefield, then the MUSIC spectrum would exhibit multiple peaks. This is illustrated in the next section.

Multisignal DF Example. The MUSIC algorithm is capable of simultaneous DF on multiple incident signals. To illustrate the capability, a linear antenna array geometry is considered with two interfering signals incident on the array (17). The antennas were deployed in a nine-element minimum redundancy array configuration and this provided an equivalent 30 element filled array measurement. The plot of Fig. 8 shows the results obtained for one signal on array end fire at 180° and a second signal at 61° off array bore sight at 151°. The signal at 151° also produced a peak at 209° due to the inherent bearing ambiguity present in a linear array. The effect of the end fire grating lobe of the antenna array is evidenced by the relatively broad peak about 180°. The signal arriving at a bearing removed from the end fire condition produced the more robust peaks observed at 151° and 209°. Although the MUSIC algorithm was able to provide DF results for both signals, these data clearly indicated that angular resolution becomes poorer for signals arriving from directions near array end fire.

A situation in which the MUSIC algorithm was unable to correctly resolve the two signals is shown in Fig. 9. In this case, the AOA separation of the two signals was 4°, and the AOAs were near array end fire, 160° and 164° respectively. The image solutions were evident at 196° and 200° azimuth. Because the AOAs were close together and near array end fire, the MUSIC algorithm was not able to resolve the two signals. Two peaks were evident in the MUSIC spectrum; however, neither one indicated an AOA correctly associated with an arriving signal. Improved AOA
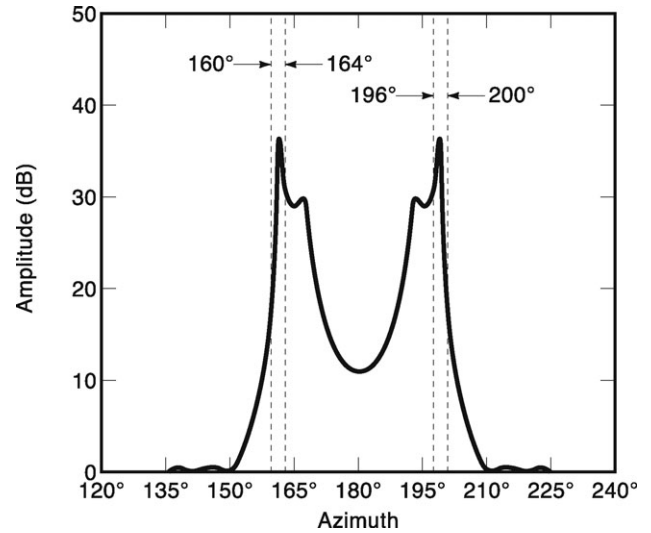
resolution can be realized for signals arriving on or near the bore sight of the array (i.e., orthogonal to the array).

Superresolution Implementation Issues. One of the primary difficulties encountered in the implementation of the superresolution techniques is the requirement for a precise characterization of the antenna array response (viz., array manifold). In general, the array manifold must be known for all frequencies, polarizations, and AOAs. In practice, an array deployed on highly conducting soil and on a site free of interacting structures may be characterized mathematically using ideal antenna responses (17). However, for antenna arrays deployed on shipboard, airborne, satellite, or other cluttered sites, a mathematical characterization is generally not possible and the array manifold must be determined by calibration using a transmitter at known locations. Due to the highly robust nature of the superresolution techniques, the array calibration must be done in increments of AOA, frequency, polarization, etc., which will be immune to significant interpolation error. These issues were discussed in the previous section relating to array calibration.

Another source of difficulty is detecting the number of signals in the wavefield. One rule-of-thumb is based on the relative magnitudes of the eigenvalues. Larger eigenvalues are associated with signals and smaller eigenvalues are associated with noise. This process works reasonably well in high SNR situations, but it is unreliable for low SNR. It has been shown that underestimation of the number of signals results in poor AOA performance (18), and for this reason, system designers generally try to overestimate the number of signals; however, overestimation may be a problem in low SNR situations due to the fact that the eigen based techniques tend to produce extraneous peaks corresponding to the number of estimated signals. A num-

ber of techniques for signal detection have been developed and one which continues to be used as a baseline for performance comparisons is the Minimum Description Length (*MDL*) criterion developed by Wax and Kailath (19).

Coherent signal interference causes a difficulty in the application of superresolution technology. The spatial covariance analysis proceeds upon the assumption that the matrix elements are a function of the separation between antennas and are not dependent upon the location of the antennas within the wavefield. If the signals are incoherent, then the spatial interference pattern will move relative to the antenna array, and the elements of the spatial covariance matrix will depend only upon the relative separation between antennas. However, if the signals are coherent, then the spatial interference pattern will be fixed in space and the elements of the spatial covariance matrix will depend both upon separation and location of the antennas. In this case, the analysis will fail. To overcome the difficulty caused by coherent interference, Shan *et al.* (20) have proposed a technique of *spatial smoothing* which partitions the antenna array into identical subsets and averages several covariance matrices of reduced size. This effectively moves the array relative to the interference pattern.

In general, the eigen decomposition part of the computation is not a significant burden, but the search for the AOA solution may be computationally intense. In particular, one must perform the matrix multiplication within Eq. (9) for each array steering vector leading to a solution. For an azimuth-only solution, the task is greatly simplified and the computational burden generally depends on the number of antennas in the array. In the case of 2-D azimuth-and-elevation AOA solutions, a number of numerical search techniques have been applied and they encounter the well known difficulties of dependence on starting point, convergence to local maxima, etc.

It should also be noted that the superresolution techniques require a radio receiver connected to each antenna to permit simultaneous sampling of the array. For this reason, superresolution implementations are frequently called N-channel systems. Multiple matched receiver channels are a major cost driver in the implementation of superresolution methods. Generally, the system designer must evaluate hardware cost versus the expected performance improvement as compared with a more conventional DF architecture consisting of a reference receiver connected to one antenna and another receiver that sequences through the remaining antennas in the array.

TRENDS IN DF RESEARCH

Two primary areas of research in the science and technology of radio direction finding are: (1) efforts to improve DF system performance in the presence of reradiating structures and (2) investigations to improve the performance of the superresolution wavefield decomposition techniques. The discussion in this section focuses on a representative subset of the many important research efforts going on.

Ongoing Developments in Array Calibration Technology

Array manifold errors arise from differences between the overall system response (i.e., including site interactions, antenna elements, interfacing networks, cabling, and characteristic impedances versus frequency) and the model from which the array manifold was derived. Errors in the array manifold generally cause DF performance degradation that equals or exceeds degradations caused by measurement errors. Array manifolds are frequently based upon the model of ideal array geometry, perfect channel amplitude/phase match, complete interelement isolation, and absence of site interaction. To the extent that these assumptions are valid, the array manifold can usually be generated analytically. When these simplifying assumptions do not apply, a conventional procedure has been to generate the array manifold through exhaustive calibration measurements with the installed array responding to cooperative transmitters, a procedure that can be expensive and/or impractical.

Because DF performance is critically dependent upon the array manifold, the development of efficient methods for accurately and completely characterizing the array manifold is a topic of active investigation. These investigations typically begin with an initial estimate of the array manifold and an assumed underlying relationship between the installed responses of the array and the initial array manifold characterization. The objective is to minimize the quantity and difficulty of controlled measurements required to accurately characterize the *installed* patterns as a function of azimuth, elevation, polarization, and/or frequency of interest. The initial array manifold characterization is analytically estimated and is assumed to be correct except for discrete, unknown factors that account for (1) antenna mutual coupling, as was done by Friedlander and Weiss (21), (2) directionally independent amplitude and phase errors, and (3) perturbations in the location of each antenna element, as proposed by Weiss and Friedlander (22).

Many research efforts seek to use a bootstrapping technique to develop a *calibrated* array manifold. In this approach, system responses are measured using signals of opportunity, and the initial estimate of the array manifold is adaptively modified to agree with the measured data. These developments usually exploit various constraints on array geometry, nature of modeling error for generating the initial array manifold estimate, knowledge and distribution of AOAs, statistical nature of the incident signal temporal characteristics, and so on. Constraints on knowledge of calibration signal AOA range from requiring complete knowledge to a complete lack of knowledge, in which case the signal AOA and the array manifold correction factors must be jointly estimated from multiple measurements of responses to the unknown signals. In a related approach, Gustafsson *et al.* (23), characterize the statistical distribution of the random differences between the initial model and the installed system response, and use this information as a basis for developing linear transformations (through weighting factors) to estimate system responses and reduce modeling errors.

Research in Superresolution Direction Finder Techniques

Detection of the Number of Signals. Since eigen DF processing is dependent on an accurate estimate of the number of signals present, research is continuing to define more effective estimation techniques. Two techniques of hypothesis testing for signal detection using eigenvalues were developed by Wax and Kailath (19) and are called the AIC and MDL methods. One of the difficulties encountered in the application of the AIC and MDL techniques is that performance tends to degrade significantly for short data rapidly as the noise back ground departs from the white Gaussian assumption. In a recent work, Chen *et al.* (24) have proposed a technique called the canonical correlation test (*CCT*) method which is designed to work well in unknown colored noise and does not require a subjective threshold setting. Also Wu and Wong (25) have developed an algorithm called parametric detection (*PARADE*), and they contend that the performance of their method is better than that of the CCT approach, particularly in the presence of correlated signals.

It has been observed that the performance of the AIC and MDL criteria tends to degrade in the presence of coherent or highly correlated signals. Ma and Teng (26) report a technique to detect the number of coherent signals through the use of a modified spatial smoothing scheme called weighted subspace smoothing (*WSS*). The authors suggest that the WSS technique provides significant performance improvement over the conventional MDL method in the presence of highly correlated or coherent signals.

Another difficulty in the application of the AIC and MDL criteria is that the performance tends to degrade significantly for short data records or in the small-sample case. This problem has been considered by Shah and Tufts (27), who propose a nonparametric procedure designed to improve performance for short data records over moderate-to-high SNRs. The authors contend that the AIC and MDL criteria do not provide flexible control over the false alarm rate while their method permits a choice of false alarm rate and corresponding probability of error. In a related work, Zhu *et al.* (28) develop two new criteria based on informational theoretic and eigen decomposition methods and an assumed noise covariance structure. The development results in modified AIC and MDL criteria which the authors claim produce significant performance improvement over the conventional AIC and MDL methods in the case of small-sample populations.

Wu *et al.* (36) derived an information-theoretic criterion for estimating the number of signals in a multi-array scenario and spatially correlated noise. Simulation results demonstrate that the approach performs well with a small number of array samples and low SNR (-0.67 dB).

A weakness of the AIC and MDL is that they explicitly assume the array manifold vectors are linearly independent. Manikas and Proukakas (36) showed that linear dependencies among array manifold vectors lead to ambiguities. An ambiguous array manifold can, under certain AOAs, create erroneous MUSIC peaks and cause the AIC and MDL to incorrectly estimate the number of signals. Abramovich *et al.* (37) address this problem by developing a sequential noise-subspace equalization (*SNSE*) detection algorithm that estimates the number of signals when the array manifold has ambiguities. The SNSE algorithm handles an overloaded array, i.e. when the number of sources exceeds the number of sensors. Simulation results showed that the SNSE performance for the overloaded array is similar to the performance of the AIC and MDL when the array is not overloaded.

Real-Time Subspace Based Implementations. Two difficulties routinely encountered in a DF operational scenario are: (1) tracking radio transmitters which are in motion and (2) the continual appearance and disappearance of radio transmissions. In both cases, there is difficulty in realizing real-time adaptive responses with the eigen based techniques since the averaging operation is used to estimate the spatial covariance matrix estimate. Averaging is necessary to obtain wide-sense stationarity and to achieve statistical stability. In a real-time signal environment, it is highly desirable to update the estimate of the number of signals present and corresponding AOAs with each new snapshot of array data.

A class of fast subspace tracking (*FST*) algorithms has been recently developed by Rabideau (29). The techniques require on the order of O(Md) operations per update (where M is the number of antennas and d is the number of estimated signals). This is contrasted with the O($M2d$) operations required in eigen decomposition methods. The author also implements a rank adaptive version of the approach called *RA-FST* which tracks changes in the number of signals present in the wavefield.

Another tracking technique has been developed by MacInnes and Vaccaro (30), and the method requires O($M2$) operations per update. The authors also propose a scheme for detecting a change in the number of signal sources using each new array snapshot. The authors contend that the new algorithm is capable of tracking rapidly changing AOAs, and that the response is virtually identical to that obtained through the use of a complete eigen decomposition at each time step. Moreover, the technique is able to accurately track appearing and disappearing sources.

Zha (31) has recently proposed the use of newly developed fast subspace decomposition methods which exploit the redundancy in large antenna arrays to reduce the computational burden of estimating AOA. The computational complexity is O(Md) + O($d3$) per data vector update.

Another proposed technique to achieve real-time implementation has been developed by performing only linear operations on the data. It is called subspace method without eigen decomposition (*SWEDE*). The technique was developed by Eriksson *et al.* (32) and is computationally simpler than the exact implementations of the eigen based methods and is also more robust to assumptions regarding noise spatial correlation. The authors assert that the approach is computationally more efficient than the approximate fast eigen decomposition algorithms, and that the computational complexity of the method is O($Md2$).

Coherent Signal Analysis. The problem of correlated signals has been attacked primarily through the application of spatial smoothing as suggested by Shan *et al.* (20). In the presence of coherent signals, the primary difficulty arises

from the fact that the spatial covariance matrix is not statistically stationary in the wide sense. That is, the terms in the matrix depend upon antenna location as well as spatial separation. Spatial smoothing is a process whereby the array is partitioned into smaller subarrays, and the resulting covariance matrices from the subarrays are averaged. The resulting averaged covariance matrix effectively *decorrelates* the coherent signals.

A technique has been recently proposed by Li *et al.* (33) to estimate AOA for coherent signal components without the use of spatial smoothing and eigen decomposition. The authors have developed a new method for 2-D spatial-spectrum estimation of coherent signals using a rectangular planar array, and the method works in the presence of unknown noise environments. The authors claim that the performance of the proposed technique is similar to that of spatial smoothing in the presence of spatially white noise, and it provides improved performance in spatially colored noise environments.

In another approach, Delis and Papadopoulos (34) propose an enhanced forward/backward spatial filtering method that provides improved performance over spatial smoothing techniques. The authors contend that their enhanced spatial filtering approach requires the same number of antenna elements as the spatial smoothing methods, and it achieves improved performance.

An improved spatial smoothing technique has been proposed by Du and Kirlin (35). Two problems with the spatial smoothing method are it reduces the effective aperture of the array, and it does not take into account the cross correlation between the subarrays. The authors propose an averaging technique which utilizes the correlations between the subarrays to produce a more statistically stable estimate of the averaged covariance matrix. The authors suggest that the technique provides improved performance when the subarrays are small compared to the size of the overall array.

If the transmitter is moving, then a concept known as temporal smoothing can be used to decorrelate coherent signals (38). Gu and Gunawan (39) showed that, for simulated VHF and UHF signals from a moving transmitter, temporal smoothing can resolve more closely spaced coherent signals than spatial smoothing. They showed temporal smoothing requires M+1 antennas to estimate the bearings of M coherent signals, whereas spatial smoothing requires 3M/2 antennas.

OPERATIONAL ISSUES

All direction finding operations proceed on the axiomatic assumption that the bearing measured is confirmed on the signal of interest. The advance of DF technology has produced DF systems with the *potential* for excellent operational performance. Experience shows this potential may never be realized in practice unless equal consideration is given to explicit *confirmation* that the AOA reported is on the signal of interest. Traditionally, DF confirmation has been the responsibility of the DF operator, while DF system engineers have concentrated on bearing accuracy, sensitivity, and response time. The growing speed and complexity of communication signals plus the need to control DF operating costs strongly favor automatic, unmanned DF operations where automatic DF confirmation is crucial for success. A review of DF confirmation techniques is beyond the scope of this article. However, DF confirmation processing is fast becoming an integral and indispensible part of DF system engineering. As a result, DF processing choices are increasingly concerned with the acquisition of signal parameter data *directly tied to the corresponding DF measurement* to confirm that the bearing is associated with the signal of interest.

BIBLIOGRAPHY

1. P. J. D. Gething, *Radio Direction Finding and Superresolution*, London: Peregrinus, 1991.

2. H. H. Jenkins, *Small-Aperture Direction-Finding*, Norwood, MA: Artech House, 1991.

3. L. F. McNamara, *The Ionosphere: Communications, Surveillance, and Direction Finding*, Malabar, FL: Krieger, 1991.

4. D. N. Travers (ed.), *Abstracts on Radio Direction Finding*, 2nd ed., San Antonio, TX: Southwest Research Institute, 1996.

5. R. E. Franks, Direction-finding antennas, *Antenna Handbook: Theory, Applications, and Design*, Y. T. Lo and S. W. Lee (eds.), New York: Van Nostrand Reinhold, 25.4–25.9, 1988.

6. D. N. Travers, Characteristics of electrically small-spaced loop antennas, *IEEE Trans. Antennas Propag.*, **13**: 639–641, 1965.

7. J. E. Hipp, Experimental comparisons of sky wave DF algorithms using a small circular array of loop antennas, *4th Int. Conf. HF Radio Syst. Techniques*, pp. 215–220, 1988.

8. H. D. Kennedy, W. Wharton, Direction-finding antennas and systems, *Antenna Eng. Handbook*, H. Jasik (ed.), New York: McGraw-Hill, 39.16–39.18, 1961.

9. J. E. Hipp, Adaptive Doppler DF system. U.S. Patent No. 5,321,410, 1994.

10. R. M. Wundt, Wullenweber arrays, *Signal Processing Arrays; Proc. 12th Symp. Agard Conf. Proc.*, Dusseldorf, (16), 128–152, 1966.

11. D. E. N. Davies, Circular arrays, *The Handbook of Antenna Design*, A. W. Rudge, K. Milne, A. D. Olver and P. Knight (eds.), London: Peregrinus, pp. 999–1003, 1986.

12. W. M. Sherrill, D. N. Travers, P. E. Martin, Phase linear interferometer system and method, U.S. Patent No. 4,387,376, 1983.

13. R. L. Johnson, Q. R. Black, A. G. Sonsteby, HF multipath passive single site radio location, *IEEE Trans. Aerosp. Electron. Syst.*, **30**: 462–470, 1994.

14. V. F. Pisarenko, The retrieval of harmonics from a covariance function, *Geophysical J. Roy. Astronom. Soc.*, **33**: 347–366, 1973.

15. R. O. Schmidt, Multiple emitter location and signal parameter estimation, *IEEE Trans. Antennas Propag.*, **AP-34**: 276–280, 1986.

16. H. Krim, M. Viberg, Two decades of array signal processing research, *IEEE Signal Process. Magazine*, **13** (4): 67–94, 1996.

17. R. L. Johnson, An experimental investigation of three eigen DF techniques, *IEEE Trans. Aerosp. Electron. Syst.*, **28**: 852–860, 1992.

18. R. L. Johnson, Eigenvector matrix partition and radio direction finding performance, *IEEE Trans. Antennas Propag.*, **AP-34**: 1986.

19. M. Wax, T. Kailath, Detection of signals by information theoretic criteria, *IEEE Trans. Acoust., Speech Signal Process.*, **ASSP-33**: 387–392, 1985.

20. T. J. Shan, M. Wax, T. Kailath, Spatio temporal spectral analysis by eigenstructure methods, *IEEE Trans. Acoust., Speech Signal Process.*, **ASSP-32**: 817–827, 1984.

21. B. Friedlander, A. J. Weiss, Direction finding in the presence of mutual coupling, *IEEE Trans. Antennas Propag.*, **39**: 273–284, 1991.

22. A. J. Weiss, B. Friedlander, Array shape calibration using eigenstructure methods, *Signal Process.*, **22**: 251–258, 1991.

23. K. Gustafsson, F. McCarthy, A. Paulraj, Mitigation of wing flexure induced errors for airborne direction-finding applications, *IEEE Trans. Signal Process.*, **44**: 296–304, 1996.

24. W. Chen, J. P. Reilly, K. M. Wong, Detection of the number of signals in noise with banded covariance matrices, *IEE Proc. Radar, Sonar Navig.*, **143**: 289–294, 1996.

25. Q. Wu, K. M. Wong, Determination of the number of signals in unknown noise environments – PARADE, *IEEE Trans. Signal Process.*, **43**: 362–365, 1995.

26. C-W Ma, C-C Teng, Detection of coherent signals using weighted subspace smoothing, *IEEE Trans. Antennas Propag.*, **44**: 179–187, 1996.

27. A. A. Shah, D. W. Tufts, Determination of the dimension of a signal subspace from short data records, *IEEE Trans. Signal Process.*, **42**: 2531–2535, 1994.

28. Z. Zhu, S. Haykin, X. Huang, Estimating the number of signals using reference noise samples, *IEEE Trans. Aerosp. Electron. Syst.*, **27**: 575–579, 1991.

29. D. J. Rabideau, Fast rank adaptive subspace tracking and applications, *IEEE Trans. Signal Process.*, **44**: 2229–2244, 1996.

30. C. S. MacInnes, R. J. Vaccaro, Tracking direction-of-arrival with invariant subspace updating, *IEEE Trans. Signal Process.*, **50**: 137–150, 1996.

31. H. Zha, Fast algorithms for direction-of-arrival finding using large ESPRIT arrays, *Signal Process.*, **48**: 111–121, 1996.

32. A. Eriksson, P. Stoica, T. Soderstrom, On-line subspace algorithms for tracking moving sources, *IEEE Trans. Signal Process.*, **42**: 2319–2329, 1994.

33. P. Li, J. Sun, B. Yu, Two-dimensional spatial-spectrum estimation of coherent signals without spatial smoothing and eigendecomposition, *IEE Proc. - Radar, Sonar Navig.*, **143**: 295–299, 1996.

34. A. Delis, G. Papadopoulis, Enhanced forward/backward spatial filtering method for DOA estimation of narrowband coherent sources, *IEE Proc. - Radar, Sonar Navig.*, **143**: 1996.

35. W. Du, R. L. Kirlin, Improved spatial smoothing techniques for DOA estimation of coherent signals, *IEEE Trans. Signal Process.*, **39**: 1208–1210, 1991.

36. Y. Wu, K. Tam, and F. Li, Determination of number of sources with multiple arrays in correlated noise fields, *IEEE Trans. Signal Process.*, **50**: 1257–1260, 2002.

37. Y. I. Abramovich, N. K. Spencer, and A. Y. Gorokhov, Detection-estimation of more uncorrelated gaussian sources than sensors in nonuniform linear antennaarrays—Part I: fully augmentable arrays, *IEEE Trans. Signal Process.*, **49**: 959–971, 2001.

38. D. R. Van Rheeden and S. C. Gupta, A temporal smoothing approach to direction of arrival estimation of coherent signals in fading channels, in *Proc. WCNC*, 286–290, 1999.

39. Z. Gu, and E. Gunawan, A performance analysis of multipath direction finding with temporal smoothing, *IEEE Signal Process. Letters*, **10**: 200–203, 2003.

RICHARD L. JOHNSON
JACKIE E. HIPP
WILLIAM M. SHERRILL
Southwest Research Institute,
6220 Culebra Road, San
Antonio, TX, 78238